



## Dynamic allometry in coastal overwash morphology

Eli D. Lazarus<sup>1\*</sup>, Kirstin L. Davenport<sup>1</sup>, Ana Matias<sup>2</sup>

<sup>1</sup>Environmental Dynamics Lab, School of Geography and Environmental Science, University of Southampton, Highfield B44, Southampton, SO17 1BJ, UK

5 <sup>2</sup>Centre for Marine and Environmental Research, University of Algarve Campus of Gambelas, Faro, Portugal

Correspondence to: Eli D. Lazarus (E.D.Lazarus@soton.ac.uk)

**Abstract.** Allometry refers to a physical principle in which geometric (and/or metabolic) characteristics of an object or organism are correlated to its size. Allometric scaling relationships typically manifest as power laws. In geomorphic contexts, scaling relationships are a quantitative signature of organisation, structure, or regularity in a landscape, even if the mechanistic processes responsible for creating such a pattern are unclear. Despite the ubiquity and variety of scaling relationships in physical landscapes, the emergence and development of these relationships tend to be difficult to observe – either because the spatial and/or temporal scales over which they evolve are so great, or because the conditions that drive them are so dangerous (e.g., an extreme hazard event). Here, we use a physical experiment to examine dynamic allometry in overwash morphology along a model coastal barrier. We document the emergence of a canonical scaling law for deposit (washover) length versus area. Comparing the experimental features, formed during a single forcing event, to four decades of change in real washover morphology from the Ria Formosa barrier system, in southern Portugal, we show that features forming at the event scale might exhibit a different pattern of change over longer time scales. This work reinforces the potential importance of initial conditions in landscape evolution, such that a landscape may reflect characteristics associated with an equilibrium or steady-state condition even when features within that landscape do not.

### 20 **1 Introduction**

In geomorphology, a scaling law is a formalised expression that typically describes how two geometric attributes of a landform relate to each other in a consistent way. Most geomorphic scaling laws take the form of a power relationship. For example, the length ( $L$ ) of a feature relative to its area ( $A$ ), as in a drainage basin (Hack, 1957; Montgomery and Dietrich, 1988), is typically expressed  $L \sim A^h$ , where the scaling exponent  $h$  defines the slope of the relationship in log-transform space. Geomorphic scaling laws derived from feature dimensions demonstrate allometry: a general physical principle in which geometric (and/or metabolic) characteristics of an object or organism are correlated to its size. Allometric patterns in geomorphology are a quantitative signature of intrinsic structure, organisation, or regularity (Church and Mark, 1980; Dodds and Rothman, 2000; Moscardelli and Wood, 2006; Straub et al., 2007; Paola et al., 2009; Wolinsky et al., 2010; Edmonds et



al., 2011), and the scaling relationships that describe them can serve as useful predictive tools – even when the processes  
30 behind the patterns are complex or unclear (Shreve, 1966; Kirchner, 1993).

During the 1970s, a critical discourse concerning the utility of geomorphic scaling laws unfolded in the academic literature.  
At issue was if, and how, power laws could provide any explanatory power for insight into physical mechanisms. Following  
Horton's (1945) pivotal observations of mathematical structure in stream networks, a variety of geomorphic scaling  
35 relationships gained traction both in drainage (Langbein et al., 1947; Leopold and Maddock, 1953; Hack, 1957; Strahler,  
1957, 1958; Melton, 1958; Gray, 1961; Leopold et al., 1964) and depositional settings (Bull, 1962; Denny, 1965). Borrowing  
primarily from biology (Huxley, 1924), but also from urban geography (Berry and Garrison, 1958) and economics (Simon  
and Bonnini, 1958), Woldenberg (1966) applied the concept of allometric growth – defined as "growth of a part at a different  
40 rate from that of a body as a whole" (Huxley and Tessier, 1936) – to the emergence of stream order within a drainage basin  
(Horton, 1945). Extension of the theory triggered an essential, not simply semantic, terminological distinction between  
allometry versus allometric growth (Mosley and Parker, 1972). The broadest conception of allometry includes all  
relationships that describe "a size-correlated change in shape" (Gould, 1966). Allometric growth, meanwhile, implies that the  
*rates* of size-correlated changes in shape describe an organised relationship. Although a test of drainage-network evolution  
in an experimental basin by Mosley and Parker (1972) did not confirm Woldenberg's (1966) argument for allometric growth,  
45 neither did their exercise disparage geomorphic allometry as a subject for further research. Rather, Mosley and Parker (1972)  
describe their null result with a generosity that further opened the problem, encouraging geomorphologists to consider the  
inductive challenges posed by "static" versus "dynamic" allometry (Mosley and Parker, 1972; Bull, 1975, 1977; Church and  
Mark, 1980).

50 The majority of geomorphic scaling laws exemplify static allometry: snapshots of landform examples sampled from a  
collection of different sites, or from a "population" of many examples at a single site. Aggregating examples in this way  
enables objective comparison across a variety of cases and contexts – for example, placing field observations and model  
results in the same parameter space, or compiling field data from different physical environments and new and historical  
observational records. However, where static allometry reflects the "interrelations of measurements made of an object at one  
55 time in its history", dynamic allometry reflects sequential measurements of shape over time (Bull, 1975). Depending on the  
landform of interest, directly observing dynamic allometry in real settings can be extraordinarily difficult: consider, for  
example, that any feature dominated by diffusion will change on a time scale proportional to the square of the feature's  
length scale,  $t \sim L^2$ . (That is, the bigger the landscape feature, the more patient an observer needs to be.) However, in  
experimental or numerical model systems, time scales of physical landscape change are deliberately accelerated and dynamic  
60 allometry can be revealed in high-frequency time series.



Here we show new evidence of dynamic allometry in overwash morphology from a previously reported physical experiment (Lazarus, 2016), documenting the progressive development of (1) a stable scaling exponent relating feature length and area, and (2) a dominant aspect ratio (or "spacing ratio") relating feature width to length (Fig. 1). From an ensemble of experimental trials that each simulated a single storm event, we measured dynamic allometry in the "population" of washover features that formed across the spatially extended experimental domain. We also investigated allometry in a sample of individual washover features that we tracked through time. To begin exploring signatures of dynamic allometry over significantly longer time scales, we examined repeated measurements of overwash morphology along the Ria Formosa barrier system, in southern Portugal, from a set of aerial images spanning five decades (Matias et al., 2008). We find a motivating correspondence between the experimental and real cases.

## 2 Data

### 2.1 Physical Experiment

Experimental data comes from orthorectified overhead images of a physical model of a coastal barrier that produced spatial sets of depositional lobes – called washover – formed by overwash flow. (Lazarus (2016) describes the experiment in detail.) The essential design consideration was geometric: a low barrier (a small difference in relative height between the barrier top and back-barrier platform) with an extended aspect ratio in the alongshore dimension. The experiment was conducted in a sediment tank (500 x 300 x 60 cm) at St Anthony Falls Laboratory (National Center for Earth-surface Dynamics, Minnesota, USA). Using well-sorted, coarse river sand (D50 ~0.59 mm), a low, rectangular, topographically smooth barrier with an extended aspect ratio (30–90 x 300 x 2 cm) was constructed across the tank, creating an "ocean" reservoir on one side and a level back-barrier plane on the other.

To run a trial, the water level in the reservoir was raised with a constant infill rate. When the reservoir water level exceeded the barrier height, flow travelled in a continuous front across the barrier top and down onto the back-barrier plane, incising overwash throats and depositing washover lobes along the back-barrier edge. Over tens of minutes, competition for available flow meant that overwash morphology developed at different rates along the barrier. The only hydrodynamic forcing came from water height relative to the barrier, making this experiment broadly representative of an "inundation regime" in the hierarchy of extreme storm impacts (Sallenger, 2000).

Flow drained at the far boundary of the back-barrier plain. Overwash flow over the barrier was observed to be subcritical, at a flow depth  $\sim \leq 1$  cm, but was locally supercritical within the throats. Note that cross-shore overwash flow in the field and in large-scale experiments tends to be supercritical (Matias et al., 2010, 2016). Trials ran until the barrier reached effective steady state, when little or no sediment movement was evident. Despite subtle indications of percolation through the back-barrier face, throats only formed in response to overwash flow, not from back-barrier slope failure or groundwater sapping. Each of the trials reported here used the same barrier height (2 cm) and infill rate ( $\sim 0.3 \text{ L s}^{-1}$ ).



95

From the overhead imagery, we used digital geospatial software to measure washover morphometry: length  $L$ , in the cross-shore dimension; width  $W$ , in the alongshore dimension; area  $A$ ; and alongshore spacing between washovers. (Previous work by Lazarus (2016) used laser-scanned topography of the final experimental condition.) Experimental washover features were approximately 10–20 cm long (length  $L$ ) in the cross-shore dimension (Fig. 1).

100

## 2.2 Field examples spanning multiple decades

Measurements of washover morphology from the Ria Formosa barrier system in southern Portugal are described in detail by Matias et al. (2008). The system includes a group of seven sandy barriers that wrap around a pronounced right-angle bend in the coastline, thus capturing two different wave exposures (to the southwest and southeast). Washover length and area were recorded from eleven sets of vertical aerial photographs taken between 1947 and 2001 for a total of 369 washover sites. In a georeferenced subset of these, the same washover sites were found in up to four images spanning multiple decades. Washover length (cross-shore distance between barrier crest and back-barrier edge) in the Ria Formosa data reached a maximum of 250 m.

110 Note that Figure 1, adapted from Lazarus (2016), shows washover measurements from Core Banks, North Carolina (USA), and a globally distributed dataset from Hudock (2013) and Hudock et al., (2014). Both datasets represent "snapshots" of population allometry, and thus help motivate this work, but they contain no repeated measurements in which to examine dynamic allometry, and so we do not re-analyse them here.

## 115 3 Results

Previous comparative analysis of field and experimental observations of overwash morphology demonstrated notable similarity in morphometric scaling (Lazarus, 2016), but looked only at "final" landform configurations (Fig. 1). Here, we present new analyses that examine the evolution of overwash morphology. We aggregated measurements from an ensemble of experimental trials and series of aerial images, respectively. No single trial nor imagery year determines the ensemble scaling relationships that we calculate (Fig. 2), nor do other contextual variables, such as barrier segment or orientation, appear to affect the collective scaling in the field measurements (Fig. S1).

120

### 3.1 "Population" allometry

A sequence of images from an experimental trial illustrates how the scaling exponent relating washover length to area, for a "population" of related washovers, changes over time during a single forcing event, also capturing the emergence of a dominant width-to-length aspect (or spacing) ratio between washovers alongshore (Fig. 3). Aspect ratio – defined as alongshore width relative to cross-shore length, or  $W:L$  – can be calculated for any individual washover. When washovers

125



are arrayed alongshore, such that neighbouring features share an edge, the aspect ratio reflects a normalised measure of spacing between adjacent deposits (Fig. 1). The same principle holds for contiguous drainage basins arrayed along quasi-linear mountain fronts (Hovius, 1996; Talling et al., 1997; Perron et al., 2009). Here, experimental washovers were initially long and narrow, yielding a high length-to-area scaling exponent (a steeply sloping fit in log-log space) and a low width-to-length aspect ratio. As a trial progressed, washovers rapidly widened – and in many cases, merged – growing in area relative to length, causing the length-to-area scaling exponent to decrease and the aspect ratio to increase.

Measuring the length-to-area scaling exponent and aspect ratio from sequential images in each experimental trial yields the evolution of these scaling metrics as a function of per cent trial run-time (Fig. 4). The populations in each trial converge on dominant scaling relationships. Because these scaling relationships are quantitative signatures of a predominant morphological expression and a preferred spatial arrangement, documenting their spatio-temporal development is a step toward connecting pattern to process. Hypothetically, the "final" scaling relationships could have been the consequence of each washover conforming to a single set of dimensional constraints from the outset, resulting in a constant scaling relationship through time. Instead, we find convergence toward a dominant pattern signature, indicative of spatial self-organisation (Lazarus and Armstrong, 2015). If washovers are initially too far apart, they widen, and some new deposits fill in between them, until the alongshore pattern reaches a closer spacing configuration. Conversely, if washovers are initially too close, they merge, effectively adjusting their centroids to be farther apart.

145

### 3.2 Dynamic allometry of individual washovers

The experiments reflect morphometric development in individual washovers during a single forcing event (Fig. 5a). The dynamic allometry of individual washovers shows that their growth trajectories are variable. In general, the washovers all grow over time, moving up the trend of the length-to-area scaling relationship if not necessarily conforming to its slope. Such variability evident at the individual level – likely an indirect reflection of morphodynamic changes occurring simultaneously to neighbouring washovers alongshore (Fig. 4) – suggests that collective convergence to a predominant scaling relationship is an emergent behaviour of the larger barrier system.

In contrast to the single forcing event of the experiments, measurements of individual washovers at Ria Formosa (Fig. 5b) reflect morphometric changes sustained over multiple decades from many forcing events and long periods of quiescence (Matias et al. 2008). Over time, the washovers shift both up and down along the length-to-area scaling relationship, suggesting that once established, a preferred spatial configuration may exert significant control on subsequent morphological change.

Washover growth – shifting up along the scaling relationship – during a decadal interval is one indication of overwash site reactivation (Hosier and Cleary, 1977). The same washover might intermittently increase its footprint with successive storm



strikes, even if its total volume might decrease through aeolian deflation (Leatherman and Zaremba, 1987). Reactivation events may also be partial or incomplete, relative to the maximum footprint at a given site.

165 Perhaps a more surprising result is where washovers shift down the scaling relationship, to a smaller but still dimensionally  
consistent size. Such dimensional adjustment could derive from depth-dependent zonation in barrier vegetation. Storm  
deposits can drive spatial heterogeneity in vegetation growth rates: vegetation buried too deeply by a storm deposit will die,  
but for some dune and marsh plant species, shallow to moderate burial can stimulate growth (Maun and Perumal, 1999;  
Gilbert and Ripley, 2010; Walters and Kirwan, 2016). Differential plant response to burial can thus determine spatio-  
170 temporal patterns in barrier vegetation cover, as the perimeter of a washover deposit may foster an envelope of new plant  
growth. Those spatio-temporal vegetation patterns in turn facilitate or inhibit pathways of sediment transport across the  
barrier (Goldstein et al., 2017). If dynamic allometry informs how washover morphology takes shape, then its growth pattern  
may also work in reverse, informing zonal patterns of depth-dependent vegetation cover that effectively reduce the  
dimensions of a washover footprint. Furthermore, gradual processes of vegetation recovery and aeolian sand deposition  
175 within the washover can progress in irregular ways related to natural topographic heterogeneity in barrier and dune  
morphology, forcing the washover to inherit morphometric characteristics unrelated to overwash and inundation processes  
(Morton and Sallenger, 2003; Matias et al., 2008).

### 3.3 Allometric growth

180 We also looked for evidence of allometric growth in the time series for the five individual washovers tracked in the  
experiment (Fig. 5a), comparing *changes* in length to the corresponding *changes* in area. Echoing Mosley and Parker (1972),  
we find no clear indication of allometric growth in washover (Fig. S2). Again, perhaps the apparent absence of any scaling in  
the rates of change is because these washovers did not grow in spatial isolation, and were instead responding to changes  
occurring in neighbouring washovers alongshore.

185

## 4 Discussion

The convergence to a quasi-equilibrium spacing between neighbouring washovers that we observe (Figs. 3 and 4) is an  
empirical complement to numerical experiments demonstrating the emergence of regular spacing in ridge-and-valley  
topography (Figure 7 in Perron and Fagherazzi, 2012). The physical basis for the regular spacing that emerges here in the  
190 coastal overwash experiment may be closely related to its upland analogue (Lazarus, 2016). In ridge-and-valley topography,  
a preferred wavelength arises from spatial competition among incipient drainages for drainage area (Perron et al., 2008,  
2009). Valleys with greater area have greater flow capture, enabling them to deepen and propagate headward as slightly  
larger drainages gain a competitive advantage over slightly smaller neighbours. Neighbouring large valleys expand  
simultaneously but the drainage area of the divide between them diminishes, ultimately inhibiting further valley growth.



195 Subtle differences in topographic gradients from one valley to the next then determine minor, intermittent changes in  
drainage area.

Perron et al. (2008, 2009) do not mirror this explanation onto depositional patterns; all material exported from their  
numerical valleys disappears from the model domain. Still, a kind of reversal of the advection–diffusion mechanism that  
200 they describe for ridge-and-valley terrain is plausible for its depositional counterpart. Our analysis only addresses the  
depositional washover patterns, but Lazarus (2016) documented the full domain of the experimental topography, including  
the spatial array of source drainages along the barrier. In the experiments, sediment was initially advected to the back-barrier,  
especially by the first pulse of inundation over the barrier top, tending to create washovers that were long and narrow (Fig.  
3). The washovers then grew laterally and gradually, as flow was forced to spread over them, diffusing fresh sediment to  
205 their margins.

Voller et al. (2012) offer a theoretical, analytical explanation for such a reversal in the flow of geomorphic "information"  
across erosional–depositional transitions, where information moves downstream in erosional settings and upstream in  
depositional ones. Their construct is one-dimensional, but sets up a two-dimensional thought experiment. In a spatially  
210 extended erosional domain, if competition for drainage area is the underlying driver of information downstream, then in a  
spatially extended depositional domain, competition for accommodation space could be the underlying driver of information  
upstream. As deposits grow, merge, and avulse into new available accommodation space, which gets more limited as  
deposition increases, they transmit that information upstream in the form of channel profiles and backwater gradients. That  
information, in turn, is registered at the base of the sourcing valley, triggering either a reduction or increase in erosional  
215 export.

In real barrier overwash conditions there is no upstream drainage-valley source – but there is a zone of onshore  
hydrodynamic forcing that, hypothetically, could feel a backwater effect or similar change in water surface gradients along  
the barrier front (Lazarus and Armstrong, 2015). The concept and construction of the experimental barrier examined here  
220 may have much in common with a study of rill formation by Izumi and Parker (1995), who show analytically why a free  
water surface over an erodible plane will develop backwater effects and Reynolds stresses that inhibit runaway incision of  
"infinitely narrow, infinitely deep" channels (Perron et al., 2008). The formation of a barrier inlet might be a case in which a  
positive feedback allows a single cross-shore transport pathway to effectively capture all available forcing flow over a large  
spatial area. However, at a larger spatial scale, dynamical interactions among groups of inlets suggest the influence of spatial  
225 competition for the prism of water created by onshore forcing (Roos et al., 2013).

The variable the dynamic allometry of individual washovers that we record (Fig. 5a) reinforces more general remark that  
Perron and Fagherazzi (2012) make regarding what convergent paths toward a state of landscape equilibrium might look like



– a concept also flagged by Bull (1975). Describing their numerical modelling example of self-organized valley spacing,  
230 Perron and Fagherazzi (2012) note that "[s]ome characteristics of the topography, such as the relief of the main drainage  
divide, reach equilibrium values much faster than the arrangement of valleys....The adjustment of individual valley locations  
involves very small gradients in erosion rates that persist for much longer." We suggest that the same applies to our cognate  
model system of coastal overwash morphology. We see the population of washovers describing allometric relationships  
(Figs. 3 and 4), and we see individual washovers reflecting that collective allometry to varying extents. To borrow, then,  
235 from Perron and Fagherazzi (2012), "this experiment also demonstrates that different landscape features can have very  
different response times, and that some can be out of equilibrium even while others appear to be close to a steady state."

### 5 Implications

Geomorphic scaling laws are typically constructed from well-developed, steady-state topography, or from a broad sample of  
240 isolated landforms. Opportunities to record stages of dynamic allometry in a landscape, from initial to "final" morphology,  
are rare – not only for individual landforms, but also for a collective "population" of spatially related landforms. As Church  
and Mark (1980) advised: "The most appealing avenue for resolution of the problem, in general, appears to lie in recourse to  
physical models. Empirical proportional relations take on a crucial role in this strategy, for they will tell us whether or not  
scale distortion (allometry) occurs between various combinations of the extensive properties of the prototype and model."  
245 Here, we use results from an experimental coastal barrier to demonstrate not only the emergence of collective allometric  
scaling relationships from spatially related washovers, but also dynamic allometry in individual washovers as they take  
shape.

Scaling laws are a consequence, not a direct measure, of physical process. The geomorphology literature includes plenty of  
250 remonstrations against the "blind" use of empirical scaling relationships as a kind of codex. In an essay written late in his  
career, geomorphologist J. Hoover Mackin remarked that "...equations read from the graphs or arrived at by other  
mechanical manipulations of the data are presented as terminal scientific conclusions. I suggest that the equations may be  
terminal engineering conclusions, but, from the point of view of science, they are statements of problems, not conclusions. A  
statement of a problem may be very valuable, but if it is mistaken for a conclusion, it is worse than useless because it implies  
255 that the study is finished when in fact it is only begun" (Mackin, 1963). Making a related argument that an allometric  
relationship is more interesting for what it frames than what it is unto itself, Bull (1977) offered: "Allometric change is not  
the mere presentation of regression analyses. It is a conceptual framework for the analysis of landforms that may allow one  
to better understand the static and dynamic interrelations between variables that tend, or do not tend, toward equilibrium".

260 A particularly strict conclusion to draw from the abstraction between the geomorphic scaling laws we can observe and the  
transport laws they imply is that scaling laws are "of scientific interest only if they can provide insight into the underlying



mechanisms" (Church and Mark, 1980). Inasmuch as scaling laws for geomorphic features (as opposed to forces) are a manifestation of geopatterns – intrinsic spatial patterns that arise in landscapes – then such insight into underlying mechanisms speaks to some of the stated grand challenges of Earth-surface processes (NRC, 2010): How do geopatterns on Earth's surface arise, and what do they tell us about process? How do local interactions give rise to extensive, organised landscape patterns? What does spatial organisation tell us about underlying processes? And beyond those questions, what are the transport laws that govern the evolution of the Earth's surface?

Morphometric scaling laws may be more useful for approaching these grand challenges than they might seem – and nowhere more directly than in geomorphic experiments. Noting "the observed consistency between experimental and field systems despite large differences in governing dimensionless numbers," Paola et al. (2009) discuss the underappreciated power of "external similarity", in which "a small copy of a system is similar to the larger system" – even if the internal physical forces that shape the former are irreconcilably different from those that shape the latter. Paola et al. (2009) argue, as have others since (Kleinhans et al., 2014; Baynes et al., 2018), that experiments that do not conform to the rules of dynamical scaling are in fact the only way to find and test the boundaries of scale dependence and independence. A small, modelled system that looks and acts like its larger, real system might not be governed by the same transport laws, but it will convey vital information about other scaling relationships that do and do not break (van Dijk et al., 2012; Kleinhans et al., 2015; Sweeney et al., 2015; Bufe et al., 2016; Lai et al., 2016; Lazarus, 2016). This advantage is philosophically related to Bull's (1977) interest in using scaling laws to reveal "variables that tend, or do not tend, toward equilibrium".

In coastal settings, especially, novel methods by which to directly measure hydrodynamics and sediment transport, particularly under storm conditions, are bringing field, experimental, and numerical studies into ever better alignment (Leatherman, 1976; Leatherman and Zaremba, 1987; Matias et al., 2010; Sherwood et al., 2014; Englestad et al., 2018; Splinter et al., 2018; Phillips et al., 2019; Simmons et al., 2019; Vos et al., 2019; Wiggins et al., 2019; Dodet et al., 2019; Wesselman et al., 2019). Within the frame of geomorphology's grand challenges, such advances make dynamic coastlines "process 'hot spots' – areas where a high level of activity concentrated in a small location can be identified from relatively simple morphologic measures", especially when "topographically based estimates...provide field scientists with a set of reference values for key local variables that serve as a starting template for observation" (NRC, 2010). Morphometric scaling relationships can be used to test numerical morphodynamic models (Lesser et al., 2004; Roelvink et al., 2009) to either confirm what the models generate or identify areas for improvement. Our work thus reiterates the utility of morphometric allometry as a window into dynamical behaviour, especially for geomorphic phenomena – such as those formed during extreme forcing events – that still confound observation *in situ*.



295 **Data Availability** – Datasets used in this work will be available via *Figshare* (link TBD).

**Author Contributions** – EDL conceived the idea, performed the experiment, and conducted the analysis. KD measured morphometry in the experiment imagery and contributed to the analysis. AM provided the Ria Formosa dataset and contributed to data interpretation. EDL drafted the manuscript, with contributions from AM and KD.

**Competing Interests** – The authors declare that they have no conflicts of interest.

300 **Acknowledgements** – EDL thanks Chris Paola for his invitation to conduct the original experiment at St. Anthony Falls Laboratory (SAFL) through the National Center for Earth-surface Dynamics Program (NCED2). EDL also thanks Chris Ellis, Jim Tucker, Aaron Bufe, Colin Phillips, Ajay Limaye, and SAFL's student work crew for advice and assistance during the experimental trials; Evan Goldstein, Vaughan Voller, Alex Densmore, Sebastian Castelltort, Dylan McNamara, Scott Armstrong, Alida Payson, and Taylor Perron for helpful discussions; and Stuart McLelland for an invitation to the 4th  
305 Hydalab+ Workshop Event, "Advanced Workshop on Scaling Morphodynamics in Time" (January, 2018; Grenoble, France). This work was supported by the NCED2 Visiting Scientist program (via NSF grant EAR-1246761), by a research grant from the British Society for Geomorphology, by the NERC BLUEcoast project (NE/N015665/2), by the EPSRC Vacation Bursary Scheme (via the University of Southampton), and by the Leverhulme Trust (RPG-2018-282). The experimental concept began on a chalkboard at the 2011 NCED Summer Institute for Earth-surface Dynamics (via NSF grant EAR-0120914). AM  
310 acknowledges the EVREST project (PTDC/MAR-EST/1031/2014), funded by the Portuguese national funding agency for science, research and technology, FCT (Fundação para a Ciência e a Tecnologia).

## References

- Baynes, E. R. C., Van de Lageweg, W. I., McLelland, S. J., Parsons, D. R., Aberle, J., Dijkstra, J., Henry, P. Y., Rice, S. P., Thom, M., and Moulin, F.: Beyond equilibrium: Re-evaluating physical modelling of fluvial systems to represent climate  
315 changes, *Earth-Sci. Rev.*, 181, 82–97, <https://doi.org/10.1016/j.earscirev.2018.04.007>, 2018.
- Berry, B. J. L., and Garrison, W. L.: Alternate explanations of urban rank-size relationships, *Ann. Assoc. Am. Geog.*, 48, 83–91, <https://doi.org/10.1111/j.1467-8306.1958.tb01559.x>, 1958.
- Bufe, A., Paola, C., and Burbank, D. W.: Fluvial bevelling of topography controlled by lateral channel mobility and uplift rate, *Nat. Geosci.*, 9, 706–710, <https://doi.org/10.1038/ngeo2773>, 2016.
- 320 Bull, W. B.: Relations of alluvial-fan size and slope to drainage-basin size and lithology in western Fresno County, California, *U.S. Geol. Surv. Prof. Pap.* 450-B, 1962.
- Bull, W. B.: Allometric change of landforms, *Geol. Soc. Am. Bull.*, 86, p. 1489–1498, [https://doi.org/10.1130/0016-7606\(1975\)86<1489:ACOL>2.0.CO;2](https://doi.org/10.1130/0016-7606(1975)86<1489:ACOL>2.0.CO;2), 1975.



- Bull, W. B.: The alluvial-fan environment, *Prog. Phys. Geog.*, 1, 222–270, <https://doi.org/10.1177/030913337700100202>,  
325 1977.
- Church, M., and Mark, D. M.: On size and scale in geomorphology, *Prog. Phys. Geogr.*, 4, 342–390,  
<https://doi.org/10.1177/030913338000400302>, 1980.
- Denny, C. S.: Alluvial fans in the Death Valley region, California and Nevada, *U.S. Geol. Surv. Prof. Pap.* 466, 1965.
- Dodds, P. S., and Rothman, D. H.: Scaling, universality, and geomorphology, *Annu. Rev. Earth Planet. Sci.*, 28, 571–610,  
330 <https://doi.org/10.1146/annurev.earth.28.1.571>, 2000.
- Dodet, G., Castelle, B., Masselink, G., Scott, T., Davidson, M., Floc'h, F., Jackson, D., and Suanez, S.: Beach recovery from  
extreme storm activity during the 2013–14 winter along the Atlantic coast of Europe, *Earth Surf. Proc. Land.*, 44, 393–401,  
<https://doi.org/10.1002/esp.4500>, 2019.
- Edmonds, D. A., Paola, C., Hoyal, D. C. J. D., and Sheets, B. A.: Quantitative metrics that describe river deltas and their  
335 channel networks, *J. Geophys. Res.-Earth*, 116, F04022, doi:10.1029/2010JF001955, 2011.
- Engelstad, A., Ruessink, B. G., Hoekstra, P., and van der Vegt, M.: Sand suspension and transport during inundation of a  
Dutch barrier island, *J. Geophys. Res.-Earth*, 123, 3292–3307, <https://doi.org/10.1029/2018JF004736>, 2018.
- Gilbert, M. E., and Ripley, B. S.: Resolving the differences in plant burial responses, *Austral Ecol.*, 35, 53–59,  
<https://doi.org/10.1111/j.1442-9993.2009.02011.x>, 2010.
- 340 Goldstein, E. B., Moore, L. J., and Durán Vinent, O.: Lateral vegetation growth rates exert control on coastal foredune  
hummockiness and coalescing time, *Earth Surf. Dynam.*, 5, 417–427, <https://doi.org/10.5194/esurf-5-417-2017>, 2017.
- Gould, S. J.: Allometry and size in ontogeny and phytogeny, *Biol. Rev.*, 41, 587–640, <https://doi.org/10.1111/j.1469-185X.1966.tb01624.x>, 1966.
- Gray, D. M.: Interrelationships of watershed characteristics, *J. Geophys. Res.*, 66, 1215–1223,  
345 <https://doi.org/10.1029/JZ066i004p01215>, 1961.
- Hack, J. T.: Studies of longitudinal stream profiles in Virginia and Maryland, *U.S. Geol. Surv. Prof. Pap.* 294-B, 45–97,  
1957.
- Horton, R. E.: Erosional development of streams and their drainage basins: hydrophysical approach to quantitative  
morphology, *Geol. Soc. Am. Bull.*, 56, 275–370, [https://doi.org/10.1130/0016-7606\(1945\)56\[275:EDOSAT\]2.0.CO;2](https://doi.org/10.1130/0016-7606(1945)56[275:EDOSAT]2.0.CO;2), 1945.
- 350 Hosier, P. E., and Cleary, W. J.: Cyclic geomorphic patterns of washover on a barrier island in southeastern North Carolina,  
*Environ. Geol.*, 2, 23–31, <https://doi.org/10.1007/BF02430662>, 1977.



- Hudock, J. W.: Barrier island associated washover fan and flood tidal delta systems: A geomorphologic analysis and proposed classification scheme for modern washover fans and examination of a flood tidal delta complex in the Cretaceous upper McMurray Formation, Alberta, Canada, M.S. thesis, University of Texas at Austin, USA, 131 pp., 2013.
- 355 Hudock, J. W., Flaig, P. P., and Wood, L. J.: Washover fans: A modern geomorphologic analysis and proposed classification scheme to improve reservoir models, *J. Sediment. Res.*, 84, 854–865, <https://doi.org/10.2110/jsr.2014.64>, 2014.
- Hovius, N.: Regular spacing of drainage outlets from linear mountain belts, *Basin Res.*, 8, 29–44, <https://doi.org/10.1111/j.1365-2117.1996.tb00113.x>, 1996.
- Huxley, J. S.: Constant differential growth-ratios and their significance, *Nature*, 114, 895–896, <https://doi.org/10.1038/114895a0>, 1924.
- 360 Huxley, J. S., and Tessier, G.: Terminology of relative growth, *Nature*, 137, 780–781, <https://doi.org/10.1038/137780b0>, 1936.
- Izumi, N., and Parker, G.: Inception of channelization and drainage basin formation: Upstream-driven theory, *J. Fluid Mech.*, 283, 341–363, <https://doi.org/10.1017/S0022112095002357>, 1995.
- 365 Kleinhans, M. G., van Dijk, W. M., van de Lageweg, W. I., Hoyal, D. C., Markies, H., van Maarseveen, M., Roosendaal, C., van Weesep, W., van Breemen, D., Hoendervoogt, R. and Cheshier, N.: Quantifiable effectiveness of experimental scaling of river-and delta morphodynamics and stratigraphy, *Earth-Sci. Rev.*, 133, 43–61, <https://doi.org/10.1016/j.earscirev.2014.03.001>, 2014.
- Kleinhans, M. G., Van Scheltinga, R. T., Van Der Vegt, M., and Markies, H.: Turning the tide: Growth and dynamics of a tidal basin and inlet in experiments, *J. Geophys. Res.-Earth*, 120, 95–119, <https://doi.org/10.1002/2014JF003127>, 2015.
- 370 Kirchner, J. W.: Statistical inevitability of Horton's laws and the apparent randomness of stream channel networks, *Geology*, 21, 591–594, [https://doi.org/10.1130/0091-7613\(1993\)021<0591:SIOHSL>2.3.CO;2](https://doi.org/10.1130/0091-7613(1993)021<0591:SIOHSL>2.3.CO;2), 1993.
- Lai, S. Y., Gerber, T. P., and Amblas, D. An experimental approach to submarine canyon evolution, *Geophys. Res. Lett.*, 43, 2741–2747, <https://doi.org/10.1002/2015GL067376>, 2016.
- 375 Langbein, W. B., et al.: Topographic characteristics of drainage basins, U.S. Geol. Surv., Water Supply Paper 968C, 1947.
- Lazarus, E. D.: Scaling laws for coastal overwash morphology, *Geophys. Res. Lett.*, 43, 12113–12119, [doi:10.1002/2016GL071213](https://doi.org/10.1002/2016GL071213), 2016.
- Lazarus, E. D., and Armstrong, S.: Self-organized pattern formation in coastal barrier washover deposits, *Geology*, 43, 363–366, <https://doi.org/10.1130/G36329.1>, 2015.
- 380 Leatherman, S.P.: Quantification of overwash processes, Ph.D. thesis, University of Virginia, USA, 1976.



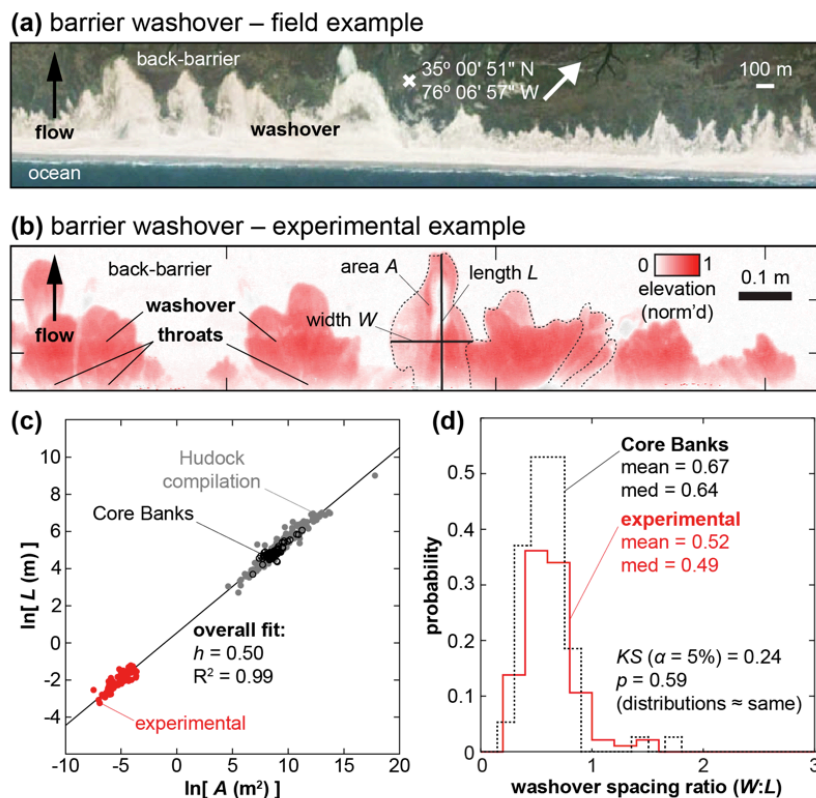
- Leatherman, S. P., and Zaremba, R. E.: Overwash and aeolian processes on a U.S. northeast coast barrier, *Sediment. Geol.*, 52, 183–206, [https://doi.org/10.1016/0037-0738\(87\)90061-3](https://doi.org/10.1016/0037-0738(87)90061-3), 1987.
- Leopold, L. B., and Maddock, T.: The hydraulic geometry of stream channels and some physiographic implications: U.S. Geol. Survey Prof. Paper 252, 1953.
- 385 Leopold, L. B., Wolman, M. G., and Miller, J. P.: *Fluvial processes in geomorphology*, W. H. Freeman, San Francisco, 1964.
- Lesser, G. R., Roelvink, J. V., Van Kester, J. A. T. M., and Stelling, G. S.: Development and validation of a three-dimensional morphological model, *Coast. Eng.*, 51, 883–915, <https://doi.org/10.1016/j.coastaleng.2004.07.014>, 2004.
- Mackin, J. H.: Rational and empirical methods of investigation in geology, in: *The fabric of geology*, edited by: Albritton, C. C., Freeman, Cooper, Stanford, California, USA, 135–163, 1963.
- 390 Matias, A., Ferreira, Ó., Vila-Concejo, A., Garcia, T., and Dias, J. A.: Classification of washover dynamics in barrier islands, *Geomorphology*, 97, 655–674, <https://doi.org/10.1016/j.geomorph.2007.09.010>, 2008.
- Matias, A., Ferreira, Ó., Vila-Concejo, A., Morris, B., and Dias, J. A.: Short-term morphodynamics of non-storm overwash, *Marine Geology*, 274, 69–84, <https://doi.org/10.1016/j.margeo.2010.03.006>, 2010.
- Matias, A., Masselink, G., Castelle, B., Blenkinsopp, C., Kroon, A.: Measurements of morphodynamic and hydrodynamic  
395 overwash processes in a large-scale wave flume. *Coastal Engineering*, 113, 33–46,  
<https://doi.org/10.1016/j.coastaleng.2015.08.005>, 2016.
- Maun, M. A., and Perumal, J.: Zonation of vegetation on lacustrine coastal dunes: effects of burial by sand, *Ecol. Lett.*, 2, 14–18, <https://doi.org/10.1046/j.1461-0248.1999.21048.x>, 1999.
- Moscardelli, L., and Wood, L.: Morphometry of mass-transport deposits as a predictive tool, *Geol. Soc. Am. Bull.*, 128, 47–  
400 80, <https://doi.org/10.1130/B31221.1>, 2016.
- Melton, M. A.: Geometric properties of mature drainage systems and their representation in an E4 phase space, *J. Geol.*, 66, 35–56, <https://doi.org/10.1086/626481>, 1958.
- Montgomery, D. R., and Dietrich, W. E.: Where do channels begin? *Nature*, 336, 232–234,  
<https://doi.org/10.1038/336232a0>, 1988.
- 405 Mosley, M. P., and Parker, R. S.: Allometric growth: a useful concept in geomorphology? *Geol. Soc. Am. Bull.*, 83, 3669–  
3674, [https://doi.org/10.1130/0016-7606\(1972\)83\[3669:AGAUCI\]2.0.CO;2](https://doi.org/10.1130/0016-7606(1972)83[3669:AGAUCI]2.0.CO;2), 1972.
- National Research Council (NRC): *Landscapes on the edge: new horizons for research on Earth's surface*, National Academies Press, Washington DC, USA, 2010.



- Paola, C., Straub, K., Mohrig, D., and Reinhardt, L.: The "unreasonable effectiveness" of stratigraphic and geomorphic  
410 experiments, *Earth Sci. Rev.*, 97, 1–43, <https://doi.org/10.1016/j.earscirev.2009.05.003>, 2009.
- Perron, J. T., and Fagherazzi, S.: The legacy of initial conditions in landscape evolution, *Earth Surf. Proc. Land.*, 37, 52–63,  
<https://doi.org/10.1002/esp.2205>, 2012.
- Perron, J. T., Dietrich, W. E., Kirchner, J. W.: Controls on the spacing of first-order valleys, *J. Geophys. Res.-Earth*, 113,  
F04016. <https://doi.org/10.1029/2007JF000977>, 2008.
- 415 Perron, J. T., Kirchner, J. W., and Dietrich, W. E.: Formation of evenly spaced ridges and valleys, *Nature*, 460, 502–505,  
<https://doi.org/10.1038/nature08174>, 2009.
- Phillips, M. S., Blenkinsopp, C. E., Splinter, K. D., Harley, M. D., and Turner, I. L.: Modes of berm and beachface recovery  
following storm reset: observations using a continuously scanning lidar, *J. Geophys. Res.-Earth*, 124, 720–736,  
<https://doi.org/10.1029/2018JF004895>, 2019.
- 420 Roelvink, D., Reniers, A., Van Dongeren, A. P., de Vries, J. V. T., McCall, R., and Lescinski, J.: Modelling storm impacts  
on beaches, dunes and barrier islands, *Coast. Eng.*, 56, 1133–1152, <https://doi.org/10.1016/j.coastaleng.2009.08.006>, 2009.
- Roos, P. C., Schuttelaars, H. M., and Brouwer, R. L.: Observations of barrier island length explained using an exploratory  
morphodynamic model, *Geophys. Res. Lett.*, 40, 4338–4343, doi:10.1002/grl.50843, 2013.
- Sallenger, A. H., Jr. (2000), Storm impact scale for barrier islands, *J. Coastal Res.*, 16, 890–895, 2000.
- 425 Sherwood, C. R., Long, J. W., Dickhudt, P. J., Dalyander, P. S., Thompson, D. M., and Plant, N. G.: Inundation of a barrier  
island (Chandeleur Islands, Louisiana, USA) during a hurricane: Observed water-level gradients and modeled seaward sand  
transport, *J. Geophys. Res.-Earth*, 119(7), 1498–1515, <https://doi.org/10.1002/2013JF003069>, 2014.
- Shreve, R. L.: Statistical law of stream numbers, *J. Geol.*, 74, 17–37, <https://doi.org/10.1086/627137>, 1966.
- Simon, H., and Bonini, C. P.: The size distribution of business firms, *Am. Econ. Rev.*, 48, 607–617, 1958.
- 430 Simmons, J. A., Splinter, K. D., Harley, M. D., and Turner, I. L.: Calibration data requirements for modelling subaerial  
beach storm erosion, *Coast Eng.*, 152, 103507, <https://doi.org/10.1016/j.coastaleng.2019.103507>, 2019.
- Splinter, K., Harley, M., and Turner, I.: Remote sensing is changing our view of the coast: Insights from 40 years of  
monitoring at Narrabeen-Collaroy, Australia, *Remote Sensing*, 10, 1744, <https://doi.org/10.3390/rs10111744>, 2018.
- Strahler, A. N.: Quantitative analysis of watershed geomorphology, *Am. Geophys. Union Trans.*, 38, 913–920,  
435 <https://doi.org/10.1029/TR038i006p00913>, 1957.
- Strahler, A. N.: Dimensional analysis applied to fluvially eroded landforms, *Geol. Soc. Am. Bull.*, 69, 279–300,  
[https://doi.org/10.1130/0016-7606\(1958\)69\[279:DAATFE\]2.0.CO;2](https://doi.org/10.1130/0016-7606(1958)69[279:DAATFE]2.0.CO;2), 1958.



- Straub, K. M., Jerolmack, D. J., Mohrig, D., and Rothman, D. H.: Channel network scaling laws in submarine basins, *Geophys. Res. Lett.*, 34, L12613, doi:10.1029/2007GL030089, 2007.
- 440 Sweeney, K. E., Roering, J. J., and Ellis, C.: Experimental evidence for hillslope control of landscape scale, *Science*, 349, 51–53, <https://doi.org/10.1126/science.aab0017>, 2015.
- Talling, P. J., Stewart, M. D., Stark, C. P., Gupta, S., and Vincent, S. J.: Regular spacing of drainage outlets from linear fault blocks, *Basin Res.*, 9, 275–302, <https://doi.org/10.1046/j.1365-2117.1997.00048.x>, 1997.
- Van Dijk, W. M., Van de Lageweg, W. I., & Kleinhans, M. G.: Experimental meandering river with chute cutoffs, *J. Geophys. Res.-Earth*, 117, F03023, <https://doi.org/10.1029/2011JF002314>, 2012.
- 445 Voller, V. R., Ganti, V., Paola, C., and Fofoula-Georgiou, E.: Does the flow of information in a landscape have direction? *Geophys. Res. Lett.*, 39, L01403, <https://doi.org/10.1029/2011GL050265>, 2012.
- Vos, K., Harley, M. D., Splinter, K. D., Simmons, J. A., and Turner, I. L.: Sub-annual to multi-decadal shoreline variability from publicly available satellite imagery, *Coast. Eng.*, 150, 160–174, <https://doi.org/10.1016/j.coastaleng.2019.04.004>, 2019.
- 450 Walters, D. C., and Kirwan, M. L.: Optimal hurricane overwash thickness for maximizing marsh resilience to sea level rise, *Ecol. Evol.*, 6, 2948–2956, <https://doi.org/10.1002/ece3.2024>, 2016.
- Wesselman, D., de Winter, R., Oost, A., Hoekstra, P., and van der Vegt, M.: The effect of washover geometry on sediment transport during inundation events, *Geomorphology*, 327, 28–47, <https://doi.org/10.1016/j.geomorph.2018.10.014>, 2019.
- Wiggins, M., Scott, T., Masselink, G., Russell, P., and McCarroll, R. J.: Coastal embayment rotation: Response to extreme events and climate control, using full embayment surveys, *Geomorphology*, 327, 385–403, <https://doi.org/10.1016/j.geomorph.2018.11.014>, 2019.
- 455 Woldenberg, M. J.: Horton's laws justified in terms of allometric growth and steady-state in open systems, *Geol. Soc. Am. Bull.*, 77, 431–434, [https://doi.org/10.1130/0016-7606\(1966\)77\[431:HLJITO\]2.0.CO;2](https://doi.org/10.1130/0016-7606(1966)77[431:HLJITO]2.0.CO;2), 1966.
- Wolinsky, M. A., Edmonds, D. A., Martin, J., and Paola, C.: Delta allometry: Growth laws for river deltas, *Geophys. Res. Lett.*, 37, L21403, doi:10.1029/2010GL044592, 2010.
- 460



465 Figure 1: This study is motivated by previous work by Lazarus (2016), from which these four panels are adapted, on  
 morphometric relationships in experimental and real coastal overwash morphology. (a) Example of coastal barrier washover  
 morphology on Core Banks (North Carolina, USA; image from 2015, via Google Earth). (b) Detail from a topographic laser scan  
 (normalized relative to maximum elevation) of experimental washover morphology, annotated with key morphometric attributes  
 (cross-shore length  $L$ , alongshore width  $W$ , area  $A$ ). (c) Log-transform relating length and area in experimental (red) and real  
 (black) washover morphology, along with measurements from Core Banks (Lazarus, 2016) and a global sample of washover  
 morphology (grey dots) from Hudock (2013) and Hudock et al. (2014). Collectively, the datasets demonstrate a power relationship  
 470 with a scaling exponent  $h = 0.50$ . (d) Stair plot comparing the alongshore spacing ratios ( $W:L$ ) of real and experimental washover  
 morphology from Lazarus (2016).

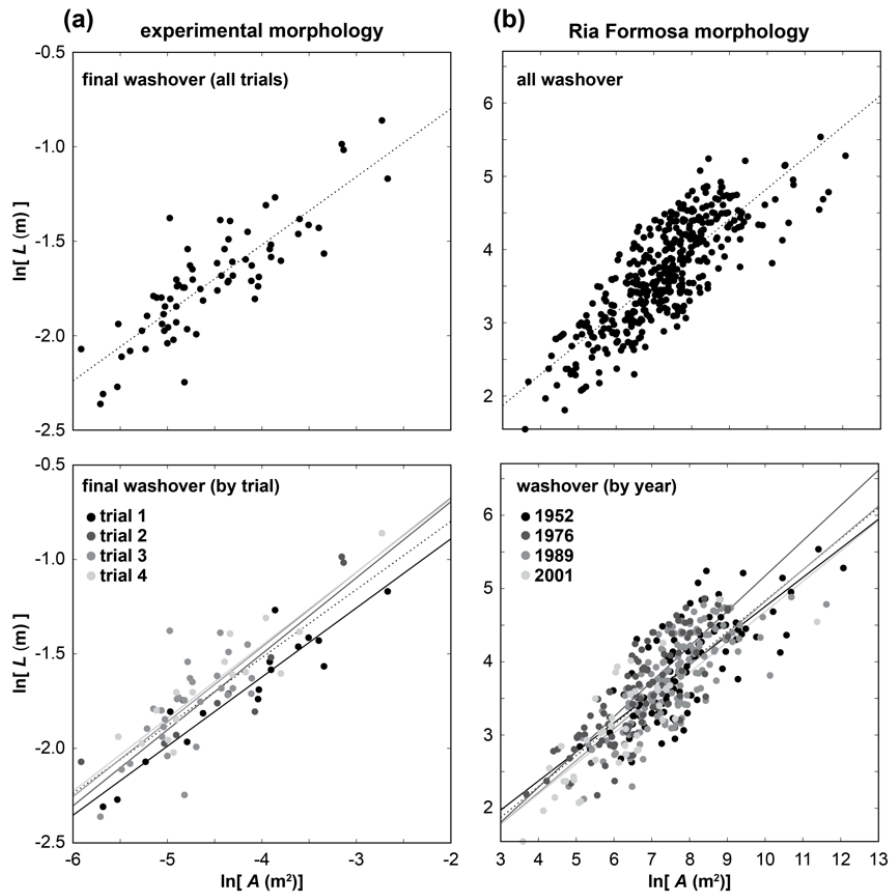
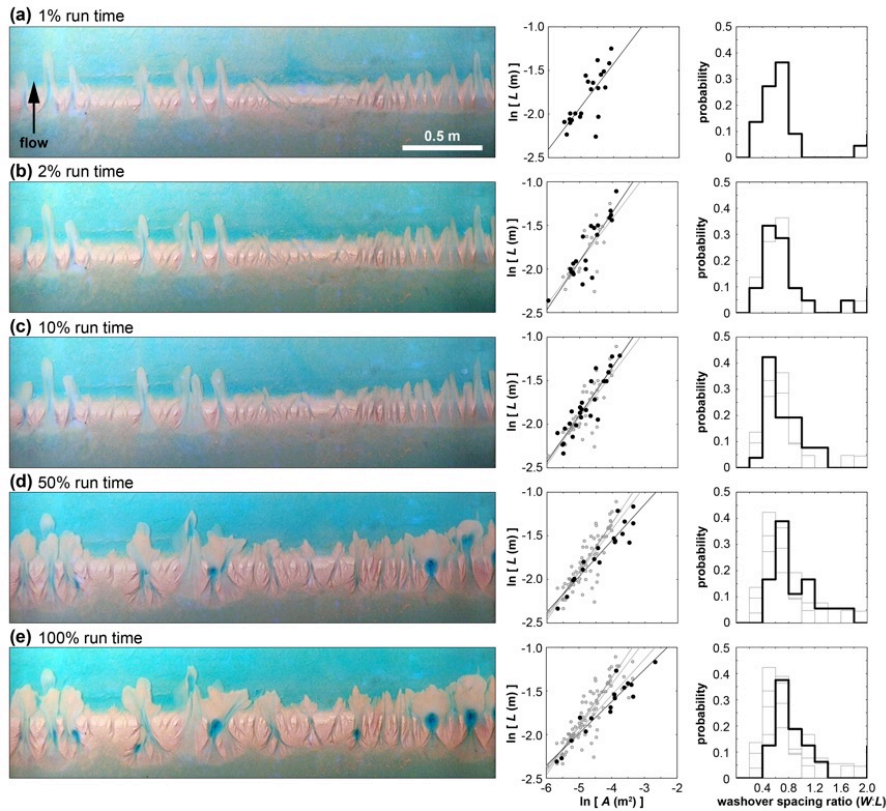
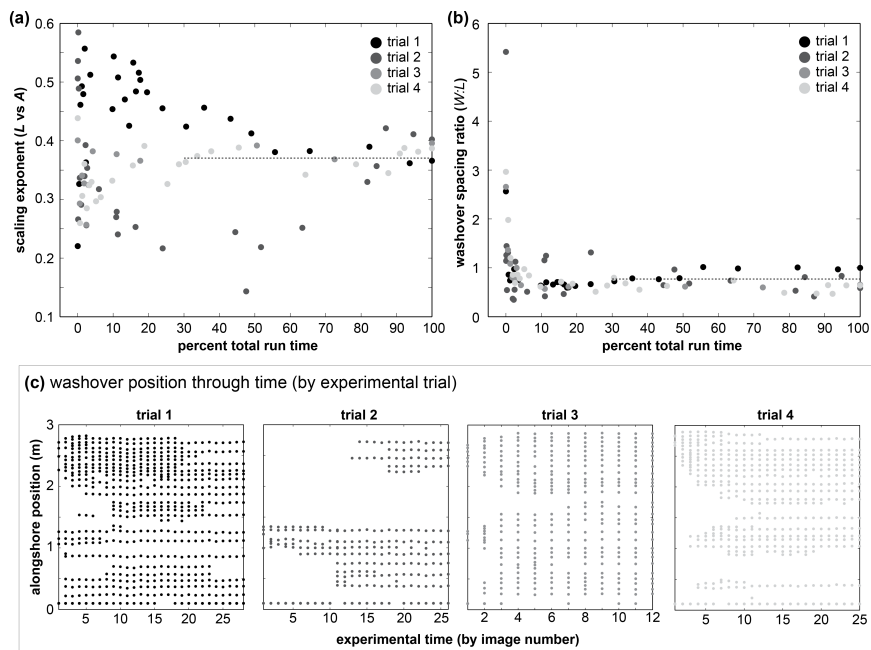


Figure 2: Log-transform comparison of length–area relationships in (a) "final", steady-state experimental washover morphology, measured from overhead imagery of the experimental tank, and (b) washovers along the Rio Formosa barriers of southern Portugal, measured from four sets of aerial images (taken in 1952, 1976, 1989, and 2001), detailed in Matias et al. (2008). Upper plots show all the data points, fitted with a power relationship. Lower plots differentiate the data according to experimental trial (left) and image year (right), each fitted with its own power relationship (along with the ensemble fits from the upper plots), demonstrating that no single trial or image year dominates the overall pattern of the data – nor does any single barrier or barrier aspect, in the Ria Formosa data (see Fig. S1). Note that the negative values for the experimental washover shown in (a) are the result of the log-transformation.



485 **Figure 3:** A demonstration of dynamic allometry in an experimental trial of overwash morphodynamics. Time is expressed as a percentage of the total run time; 100% run time reflects the "final", steady-state morphology. Overhead images of the experimental tank (left column) show, in snapshots, the washover morphology evolving as the trial progresses (a–e). Log-transform plots of washover length relative to area (middle column) show how the scaling exponent  $h$  changes through time. Data points and the fitted power relationship for a given image are plotted in black; data from previous snapshots are retained in grey. Stair plots (right column) track the related development of a preferred spacing ratio (calculated as  $W:L$ ), where the distribution at each snapshot is shown in black, and distributions from previous snapshots are retained in grey.



490 **Figure 4:** Evolution of a (a) mean scaling exponent  $h$  and (b) preferred spacing ratio ( $W:L$ ) compiled from four experimental trials  
 of overwash morphodynamics (detailed in Fig. 3). Dotted lines in (a) and (b) show respective ensemble means calculated between  
 20% and 100% run time. Panels in (c) show progressive washover position (see Fig. 2b) in each of the four experimental trials. To  
 emphasize how washover positions shift laterally before finding a morphological steady-state – the preferred spacing shown in (b)  
 – the bottom axis reflects image sequence rather than absolute time.

495

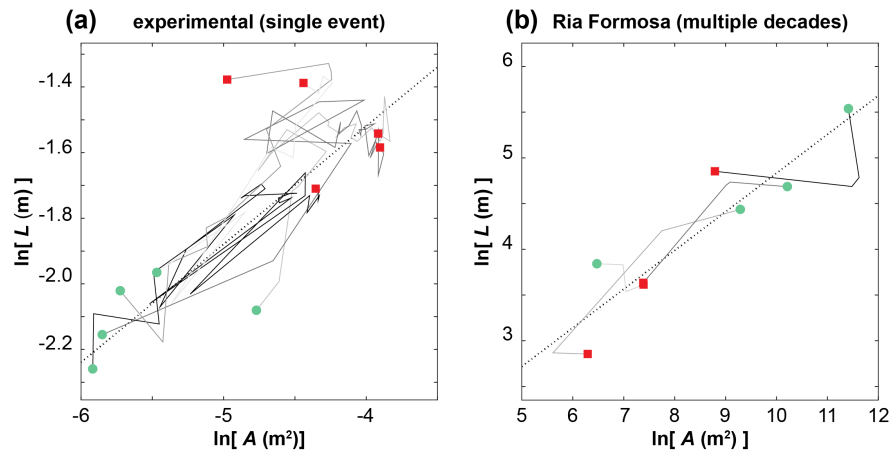


Figure 5: Dynamic allometry in a sample of individual washovers tracked (a) during the physical experimental trials, representing a single forcing event ( $n = 5$ ), and (b) identified in the four decades of aerial photographs from Ria Formosa ( $n = 4$ ). Circles and squares indicate first and last measurements in the sequence, respectively. Individual trajectories are differentiated by shade (greyscale). Fits are ensemble means from Fig. 3, and listed in Table 1.

500



**Table 1: Scaling exponents and distribution statistics.**

figure & panel	data series	scaling exponent ( $h$ )	mean spacing ratio ( $W:L$ )	median spacing ratio ( $W:L$ )
1c	overall fit	0.50		
1d	Core Banks		0.67	0.64
1d	experimental		0.52	0.49
2a	experimental (all)	0.36		
2a	trial 1	0.37		
2a	trial 2	0.40		
2a	trial 3	0.40		
2a	trial 4	0.39		
2b	Ria Formosa (all)	0.42		
2b	1952 set	0.40		
2b	1976 set	0.43		
2b	1989 set	0.48		
2b	2001 set	0.42		
3a	trial 1 @ 1% run time	0.49	0.74	0.51
3b	trial 1 @ 2% run time	0.56	0.80	0.52
3c	trial 1 @ 10% run time	0.54	0.62	0.57
3d	trial 1 @ 50% run time	0.41	0.79	0.65
3e	trial 1 @ 100% run time	0.37	1.0	0.69
4a	mean (30–100% time)	0.37		
4b	mean (30–100% time)		0.77	
5a	experimental (from 2a)	0.36		
5b	Ria Formosa (from 2b)	0.42		